3rd International Symposium on Therapeutic Ultrasound 22 – 25 June, 2003 Lyon, France
Editors: J.Y. Chapelon and C.Lafon. 186-191.

Radiation-Force Monitoring of HIFU Lesions: Effects of System and Tissue Factors

Frederic L. Lizzi[1], Samuel Mikaelian[1], Robert Muratore[1], S. Kaisar Alam[1], Sarayu Ramachandran[1], and Cheri X. Deng[2]

[1]*Riverside Research Institute, 156 William Street, New York, New York, USA*
[2]*Case Western Reserve University, Cleveland, Ohio, USA*

Abstract. Therapeutic lesions produced by high-intensity focused ultrasound (HIFU) are not always detectable using conventional ultrasonic imaging techniques. We are investigating an alternative means to detect these lesions and thereby monitor and control their production. The method senses local tissue stiffness, which increases in HIFU lesions. A therapy transducer is used to launch a short exposure, designed to produce small internal tissue motion (due to radiation force) without altering tissue structure. A co-linear diagnostic transducer tracks the induced motion and characterizes its magnitude and rise and fall times. The procedure is conducted before an intense HIFU exposure, to establish baseline tissue stiffness. It is then repeated during and following HIFU exposures to monitor stiffness changes associated with lesion development.

Our theoretical analyses and experiments address a number of issues that affect this technique. The intensity and beam properties (width, etc.) of the motion-producing beam affect the degree and time-course of induced motion. As described in this report, several tissue properties also affect induced motion. These factors include lesion geometry, Young's modulus, and acoustic absorption and attenuation coefficients. Absorption and attenuation directly affect the induced radiation-force pattern, and therefore also influence motion. This effect is important since absorption and attenuation coefficients can increase during lesion production. The current results show how these coefficients can affect the degree and spatial motion patterns within HIFU lesions. Results of the model are being used to help in data interpretation and to design push exposures to enhance lesion detection.

INTRODUCTION

Monitoring lesions produced by high-intensity focused ultrasound (HIFU) is important for precise control during therapy. Diagnostic ultrasound would seem to offer many advantages for on-line, non-invasive lesion monitoring. Diagnostic ultrasound can image "severe" lesions that involve gas-body formation due to degassing, cavitation, or vaporization. However, many therapeutic applications call for "milder" thermal lesions that involve thermal denaturation and necrosis without the production of gas bodies, which can shield distal tissues from the HIFU beam and also cause tissue alterations that are difficult to control [1]. Mild lesions have proven difficult to detect with conventional ultrasound imaging techniques.

The current study investigated a technique that employs ultrasound procedures to detect mild thermal lesions by virtue of their increased stiffness, which has been reported by several investigators [2]. As in the diagnostic-ultrasound method described

by Nightingale *et al.* [3], our technique evaluates motion induced by radiation force to evaluate tissue stiffness. Our system [4] employs a brief exposure (several milliseconds) from the therapy transducer to induce this motion, and it tracks tissue displacement by analyzing A-mode signals acquired from a central collinear diagnostic transducer. The procedure is performed prior to a therapy exposure, to determine initial stiffness characteristics. The measurement is repeated following the therapy exposure in order to detect stiffness changes associated with lesion formation.

Our initial analysis of the tissue, transducer, and system factors involved with this technique as well as our *in-vitro* experiments supported the feasibility of this method [4,5]. The current simulation studies were undertaken to further clarify the roles of several of these factors. This report describes part of our studies that examined how acoustic attenuation within a lesion affects the induced radiation-force pattern and, therefore, alters motion features. This topic is important because the attenuation and absorption are increased in thermal lesions [6]. We also examined the effect of the beam pattern used to induce the radiation force. This is an important design consideration because this beam pattern can be controlled by using selected sub-apertures of the therapy array and by varying its excitation frequency.

PRINCIPLES OF OPERATION

The operation of the radiation-force technique is indicated in Fig. 1, which shows the initial transducer configuration used in our studies. The transducer assembly contains two collinear transducers. The outer spherical-cap transducer serves as a HIFU therapy device and also is used to produce brief "push" exposures. It is fabricated from PZT and has a 90-mm focal length (radius of curvature). Its outer diameter is either 42 or 80 mm, and it is operated at its fundamental frequency (near 1.4 MHz) or its third harmonic frequency (near 4.1 MHz). The therapy transducer has a central 20-mm aperture that houses a central diagnostic transducer; this broadband transducer has a center frequency of 7.5 MHz and is positioned so that its focal point coincides with that of the therapy transducer.

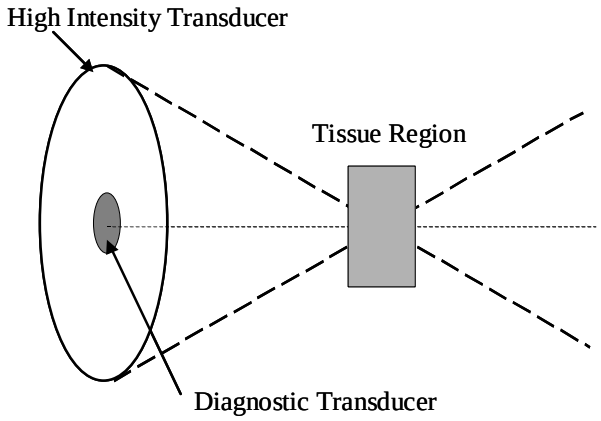

FIGURE 1. Schematic of transducer configuration.

In operation, the A-mode transducer is used to acquire radio-frequency (RF) echo data within the tissue region to be treated; these data establish the initial positions of tissue elements. The therapy transducer is then excited to deliver a brief (1-5 ms) "push" pulse that induces a radiation force within the tissue. The force produces corresponding tissue motion on the order of 1 to 10 μm. At the end of the push pulse, A-mode data are again acquired in M-mode fashion as the displaced tissue elements return towards their initial positions. Cross-correlation algorithms are then used to analyze the pre- and post-push data to compute tissue displacement as a function of time [4,5].

The displacement curves computed at sequential tissue depths are then stored to document the pre-treatment motility pattern in tissue. The therapy transducer is then excited to produce a thermal lesion using longer durations (e.g., several seconds) than those used to induce motion. Following therapy exposures, the radiation-force sequence (A-mode, push pulse, A-mode) described above is repeated to again ascertain tissue displacement as a function of time.

Lesions are detected because they introduce spatio-temporal departures from pre-treatment displacement results. Most often, lesions are apparent from the reduction of peak displacement (e.g., by 20% as in [4]). Other features being examined include recovery time constants and spatial shadowing of motion posterior to the lesion as described below.

Our previous simulation results and experiments have found that detectable motion can be produced by push pulses of several hundred W/cm^2 applied for 1 to 5 milliseconds. The corresponding temperature increases are calculated to be less than 0.1°C, well below levels for thermal damage [4,5].

SIMULATION METHODS AND RESEARCH

The current simulations studied the motion patterns induced in normal and lesioned tissue. This report describes a typical case using 4.09-MHz exposures from a transducer (Fig. 1) with a 42-mm outer diameter and a 90-mm focal length. The push pulse had a 1-ms duration and a focal-point intensity (free-field) of 345 W/ cm^2. We computed the free-field intensity $I_0(\boldsymbol{x})$ of this beam using numerical evaluation of standard diffraction integrals in homogeneous media; the vector $\boldsymbol{x}$ specifies position coordinates (x,y,z) where x denotes axial range from the transducer. The free-field beam pattern exhibited a focal-plane beam width (-3 dB) of approximately 0.8 mm. We then computed the *in-situ* beam pattern within a "normal" tissue segment centered in the focal plane; the tissue had a range extent of 30 mm and a cross-range width of 35 mm. The *in-situ* intensity $I(\boldsymbol{x})$ was calculated as $I_0(\boldsymbol{x})\ \exp(-2\alpha f x)$ where f is frequency (MHz) and the pressure attenuation coefficient α was set to 0.058 nepers/ cm-MHz.

Radiation force $F(\boldsymbol{x})$ was calculated as $2\ \alpha_{abs}\ f\ I(\boldsymbol{x})/\ c$ where c is the speed of sound (1,550 m/s) and the pressure absorption coefficient (nepers/cm-MHz) α_{abs} is set to equal 75% of the attenuation coefficient α.

The displacements resulting from the radiation force were calculated from the coupled equations of motion in elastic media. Young's modulus was set at 1.2 kPa for

normal tissue; all tissues were assigned a Poisson's ratio of 0.495. We used finite difference algorithms to compute radial and axial displacements as functions of time t and space $\boldsymbol{x}$; the axial displacement components D($\boldsymbol{x}$,t) are larger by an order of magnitude and are reported here. In the focal zone, these components give rise to shear waves because they predominantly spread radially away from the transducer axis; thus, they propagate in a direction perpendicular to the constituent particle motion, which is parallel to the transducer axis. An important observation is that such waves travel relatively slowly [7]; for the normal-tissue parameters in this study, the velocity is computed as approximately 0.6 mm/ms.

We computed displacements in homogeneous normal tissue and also in normal tissue with a central ellipsoidal lesion of axial length 6 mm and cross-range diameter 2 mm. The lesions were characterized by an elevated stiffness (Young's modulus of 6.0 kPa). We examined a series of lesion attenuation coefficients α_n set equal to multiples (n) of the normal-tissue value α; *i.e.*, $\alpha_n = n\,\alpha$, where n ranged from 1 to 6. In each case, the absorption coefficient was set equal to $0.75\,\alpha_n$.

Figure 2 shows the computed normalized radiation force along the transducer axis for normal tissue and for cases with lesions. The force for the normal case is the same as that for the lesion case with n = 1 since they have the same absorption and attenuation coefficients. As n increases, the radiation force at the anterior lesion surface progressively increases in an abrupt manner because the multiplicative absorption coefficient increases at the lesion boundary. However, the force within the lesion decreases in a more rapid manner as n increases because the larger attenuation coefficients increase the rate of exponential fall-off in *in-situ* intensity.

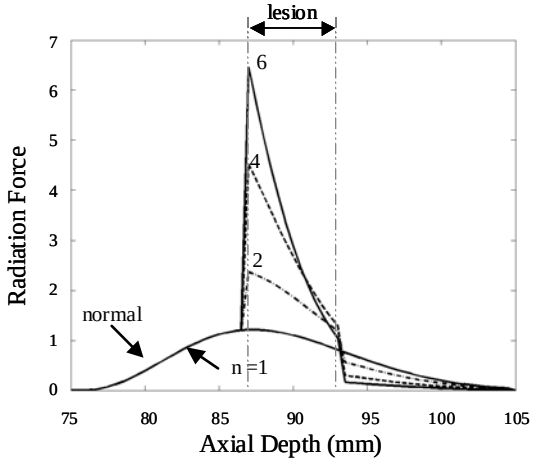

FIGURE 2. Radiation force as a function of axial distance.

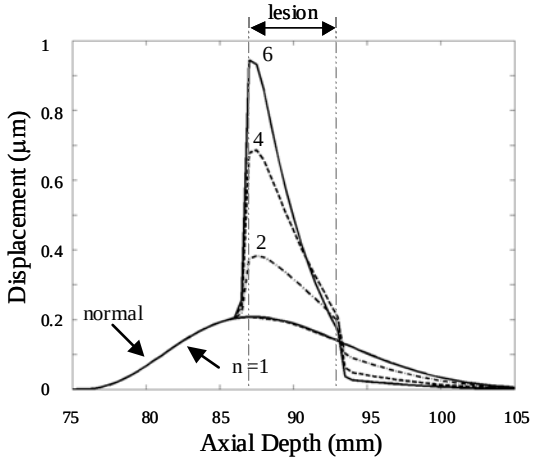

FIGURE 3. Axial displacement as a function of axial distance at 0.1 ms.

Figure 3 shows computed axial displacements along the transducer center line at 0.1 ms after the push pulse is initiated. At this short time interval, the displacement pattern for each case closely resembles the corresponding radiation force result of Fig. 2. This similarity is due to the fact that tissue segments are responding in an inertial

manner to local forces; elastic coupling to distant regions has not yet been established due to the slow propagation speed noted above.

Figure 4 shows computed axial displacements at 1.0 ms, just as the push beam is turned off. At this longer time, elastic coupling has become more significant, and the elevated Young's modulus in the lesions clearly affects their displacement patterns. The normal tissue result shows a smooth variation with position while the lesion with equal attenuation (n = 1) shows a substantial reduction in displacement within the extent of the lesion. As n increases, displacements in the anterior segments of the lesions also increase, due to the elevated anterior forces shown in Fig. 2. At the same time, motion in posterior lesion segments and in tissue behind the lesions decrease, due to the smaller forces in these segments as shown in Fig. 2.

Figure 5 plots the normalized focal-point displacement at 1 ms as a function of n. As n increases, there is a corresponding increase in displacement, but the rate of increase slows for high n. This occurs because of the competing effects of absorption and attenuation. Increased absorption coefficients increase the radiation force uniformly through the lesion: increased attenuation decreases the force progressively with lesion depth. The motion tends towards a limiting value because most of the incident beam has been attenuated at large n.

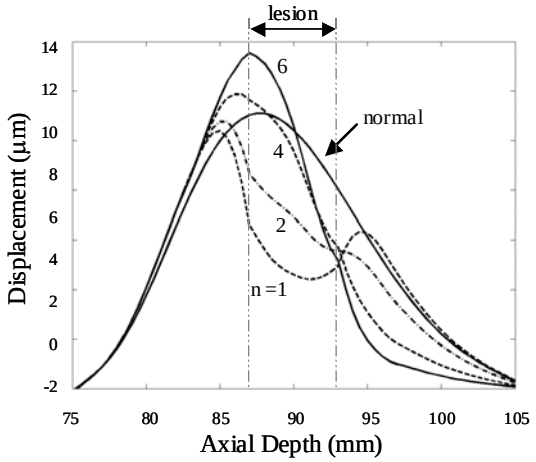

FIGURE 4. Axial displacement as a function of axial distance at 1.0 ms.

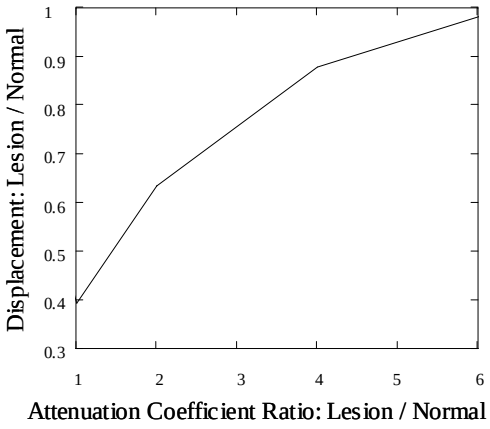

FIGURE 5. Relative axial displacement at focal point *vs.* relative lesion attenuation coefficient, at 1.0 ms.

DISCUSSION

This report described one segment of our overall studies of radiation-force techniques for lesion monitoring. The results show that the acoustic attenuation changes within lesions can affect the induced tissue motion that is sensed with diagnostic transducers. At very short times (~ 0.1 ms) after the radiation pressure is applied, induced-motion patterns closely resemble the radiation force; thus, the attenuation changes cause the same effects on the force and initial motion. At longer times (~ 1 ms), elastic coupling becomes significant and the motion is also influenced by the higher Young's modulus in the lesion. Additional studies in our laboratories

have shown that, at these longer times, motion is also influenced by the cross-range profile of the incident beam and by the lateral lesion boundaries.

The cases described in this report are consistent with our other findings in several regards. The results show that measurable motion can be induced with "push" beams that do not cause significant temperature rises. They also show that stiff lesions cause measurable changes in motion patterns, but the nature and magnitude of the changes are partly determined by the lesion attenuation coefficient. For example, this report showed how increased lesion attenuation can enhance motion in the anterior lesion segment and decrease it in the posterior segment of the lesion and in deeper tissues. Simulation studies such as in this report should help in interpreting such changes and in designing beam patterns to enhance lesion detection.

The results presented above and in previous reports support the feasibility of using the radiation-force technique to monitor thermal lesions and indicate how it is readily incorporated into therapeutic transducer assemblies. We are currently implementing this technique in a new system that uses concentric diagnostic and therapeutic arrays to provide greater versatility in applying this and related techniques.

ACKNOWLEDGMENTS

Portions of this research were supported by grant CA84588 awarded by the National Cancer Institute and the National Heart, Lung, and Blood Institute and by grant EY10369 awarded by the National Eye Institute.

REFERENCES

1. Lizzi, F.L., *Eur. Urol.*, **23**, 23-28 (1993).
2. Kallel, F., Stafford, R.J., Price, R.E., et al., *Ultrasound Med. Biol.*, **25**, 641-647 (1999).
3. Nightingale, K.R., Palmer, M.L., Nightingale, R.W., and Trahey, G.E., *J. Acoust. Soc. Am.*, **110**, 625-634 (2001).
4. Lizzi, F.L., Deng, C.X., Muratore, R., Ketterling, J.A., Alam, S.K., and Mikaelian, S., "Radiation-Force Motion Technique for Monitoring HIFU Exposures", in *Conference Proceedings of the 2nd International Symposium on Therapeutic Ultrasound*, edited by M.A. Andrew et al., Seattle: Center for Industrial & Medical Ultrasound, University of Washington, 2002, pp. 267-274.
5. Lizzi, F.L., Muratore, R., Deng, C.X., Ketterling, J.A., Alam, S.K., Mikaelian, S. and Kalisz, A., *Ultrasound Med. Biol.*, (in revision).
6. Damianou, C.A., Sanghvi, N.T., Fry, F.J., and Maass-Moreno, R., *J. Acoust. Soc. Am.*, **102**, 628-634 (1997).
7. Sarvazyan, A.P., Rudenko, O.V., Swanson, S.D., Fowlkes, J.B., and Emelianov, S.Y., *Ultrasound Med. Biol.*, **24** 1419-1435 (1998).